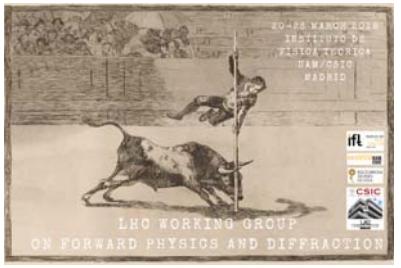

Rapidity dependence of hadroproduction of φ-mesons at LHC energies

Carlos Merino

University of Santiago de Compostela

Galiza-Spain

in collaboration with

G.H. Arakelyan and Yu.M. Shabelski

carlos.merino@usc.es

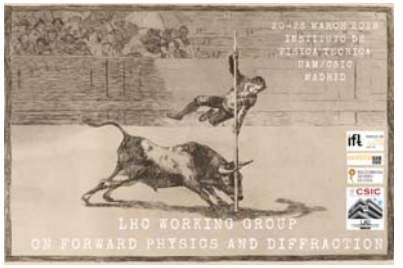

Outline:

I. Aim
II. Meson production in the Quark-Gluon String Model: inclusive spectra in pp, pA, and AA collisions
III. Description of experimental data on hadroproduction of φ-mesons on proton target.
IV. Production of φ-mesons on nuclear targets up to RHIC energies
V. Rapidity spectra of φ-mesons in pPb and PbPb collisions at LHC energies
VI. Conclusions

Phys. Rev. D90, 114019 (2014), Phys. At. Nucl. 80, 1197 (2017), and references therein

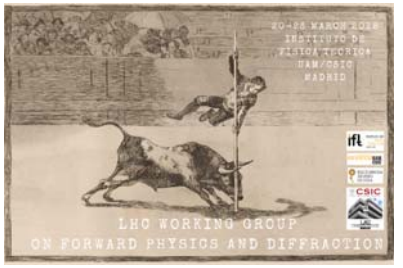

I. Aim:

To calculate in the frame of the Quark-Gluon String Model (QGSM) the spectra of secondary φ-mesons in hadron-nucleon, pA, and AA collisions for a wide energy region up to the LHC range.

Experimental data in pA and AA collisions show small shadowing corrections to the inclusive φ-meson in the midrapidity region.

The results of the QGSM calculations are in qualitative agreement with the experimental data.

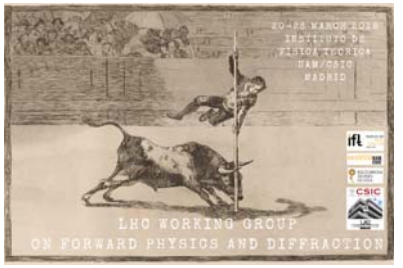

II. Meson production in the Quark-Gluon String Model: inclusive spectra in pp, pA, and AA collisions

The QGSM is based on Dual Topological Unitarization, Regge Phenomenology, and nonperturbative features of QCD.

The QGSM successfully describes multiparticle production in hadron-hadron and hadron-nucleus collisions.

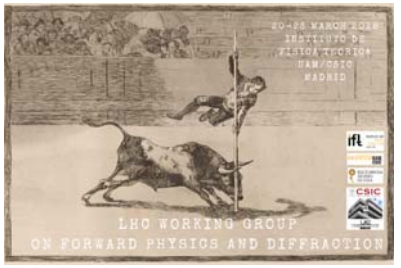

High energy interactions proceed via the exchange of one or several Pomerons, and elastic and inelastic processes result from cutting between or through Pomerons.

The inclusive spectra of hadrons are related to the corresponding fragmentation functions of quarks and diquarks, constructed by using Reggeon counting rules.

For the description of interactions with a nuclear target, the Gribov-Glauber theory is used. The interaction is considered as the superposition of interactions with different numbers of target nucleons.

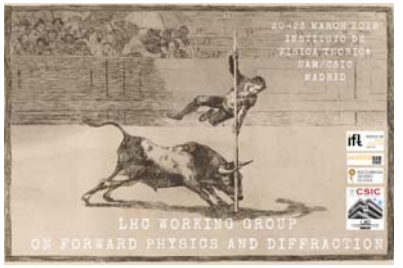

The inclusive spectrum of a secondary hadron **h** is determined by the convolution of the diquark, valence quark, and sea quark distributions, **u(x, n)**, in the incident particles, with the fragmentation functions, $G^h(z)$, of quarks and diquarks into the secondary hadron **h**.

Both the distributions and the fragmentation functions are constructed using the Reggeon counting rules.

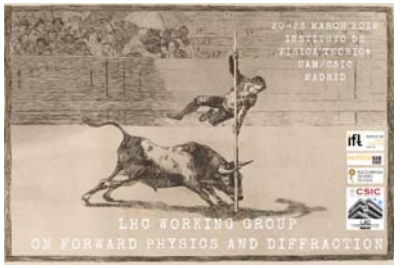

Each exchanged Pomeron corresponds to a cylindrical diagram.

When cutting one Pomeron, two showers of secondaries are produced

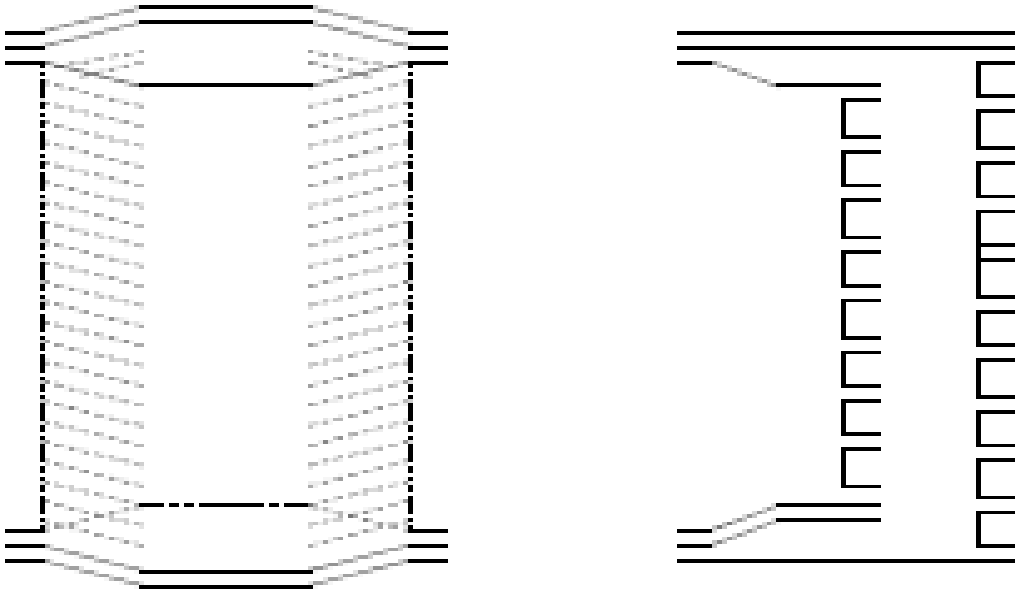

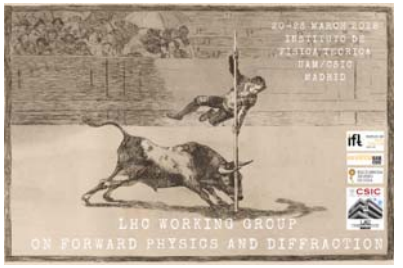

In the case of multipomeron exchange, the distributions of valence quarks and diquarks are softened due to the appearance of a sea quark contribution.

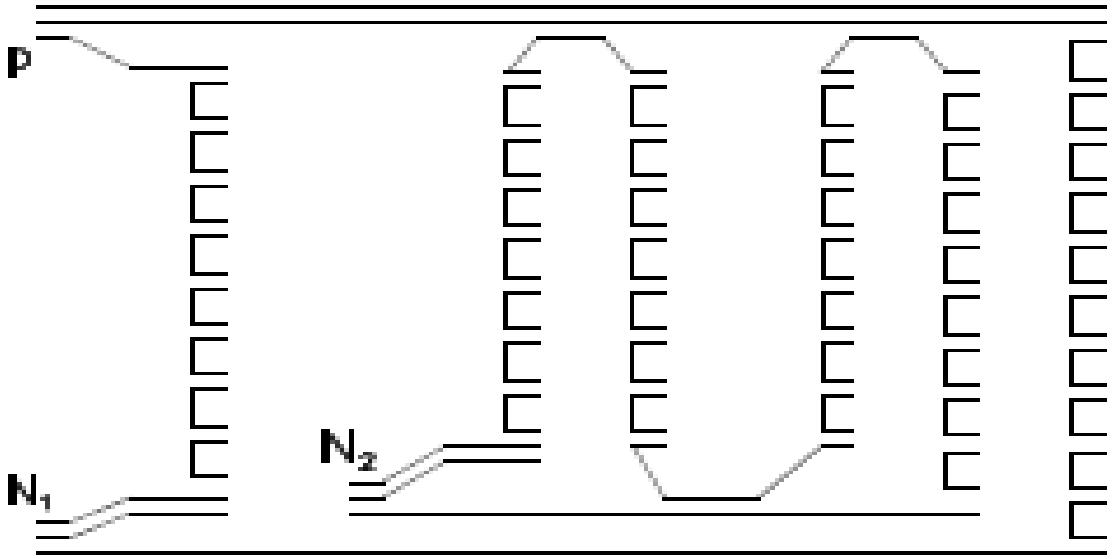

Every distribution $u_i(x, n)$ is normalized to unity.

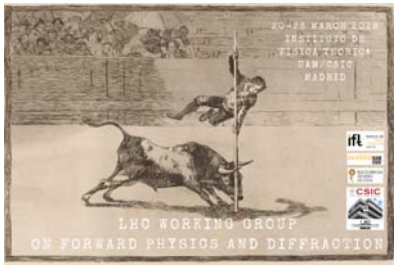

For a nucleon target, the inclusive rapidity, y, or Feynman-x, x_F , spectrum of a secondary hadron h has the form

$$\frac{dn}{dy} = \frac{x_E}{\sigma_{inel}} \cdot \frac{d\sigma}{dy} = \sum_{n=1}^{\infty} \omega_n \cdot \Phi_n^h(x)$$

where the functions $\Phi_n^h(x)$ determine the contribution of diagrams with n cut Pomerons, ω_n is the relative weight of these diagrams (we neglect the numerically small contribution of diffraction dissociation processes).

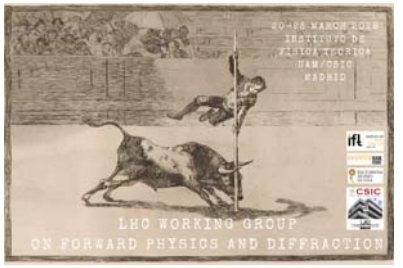

For pp collisions:

$$\phi_n^h(x) = f_{qq}^h(x_+,n)\cdot f_q^h(x_-,n) + f_q^h(x_+,n)\cdot f_{qq}^h(x_-,n) + 2(n-1) f_s^h(x_+,n)\cdot f_s^h(x_-,n) \ ,$$

$$x_\pm = \frac{1}{2}\left[\sqrt{4m_T^2/s + x^2} \pm x\right] \ ,$$

where f_{qq}, f_q, and f_s are the contributions of diquarks, valence quarks, and sea quarks, respectively.

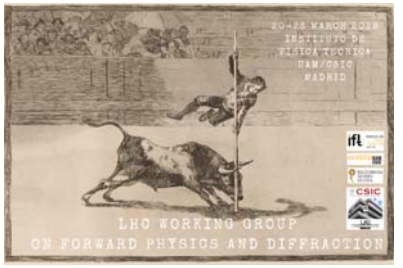

These contributions are determined by the convolution of the diquark and quark distributions with the fragmentation functions, e.g.,

$$f_q^h(x_+, n) = \int_{x_+}^1 u_q(x_1, n) \cdot G_q^h(x_+/x_1) dx_1 \quad .$$

The diquark and quark distributions, as well as the fragmentation functions are determined by Regge asymptotics.

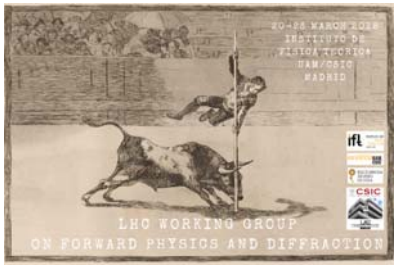

The classical Reggeon diagram technique constructs the amplitude for hadron-hadron scattering at high energies of multi-Pomeron exchanges.

In the case of supercritical Pomeron with

$$\alpha_P(t) = 1 + \Delta + \alpha'_P t, \qquad \Delta > 0,$$

one obtains the correct asymptotic behavior, $\sigma_{\text{tot}} \sim \ln^2 s.$

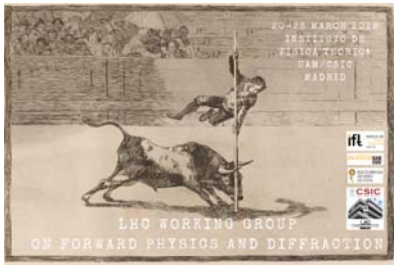

The contribution of the screening multi-Pomeron discontinuities to the total cross section can be treated in a simple quasieikonal way.

The values of the Pomeron parameters were fixed by performing a Regge fit to the experimental data on hadron-nucleon scattering up to the colliders energies:

$$\Delta = 0.139, \qquad \alpha'_P = 0.21\ \text{GeV}^{-2},$$
$$\gamma_{pp} = 1.77\ \text{GeV}^{-2}, \qquad R^2_{pp} = 3.18\ \text{GeV}^{-2},$$
$$C_{pp} = 1.5, \qquad \gamma_{\pi p} = 1.07\ \text{GeV}^{-2},$$
$$R^2_{\pi p} = 2.48\ \text{GeV}^{-2}, \qquad C_{\pi p} = 1.65.$$

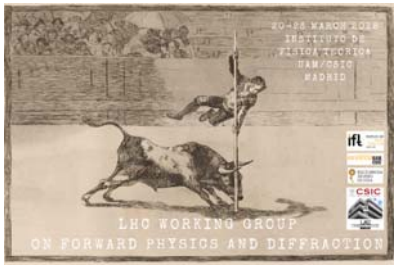

The cross sections of all inelastic processes corresponding to diagrams where n ≥ 1 Pomerons are cut can be calculated by using the AGK rules:

$$\sigma_{hN}^{(n)} = \frac{\sigma_P}{n \cdot z}\left(1 - e^{-z}\sum_{k=1}^{n-1}\frac{z^k}{k!}\right)$$

The probabilities ω_n are determined as:

$$w^n = \sigma^n / \left(\sigma^{\text{tot}} - \sigma^{\text{el}}\right)$$

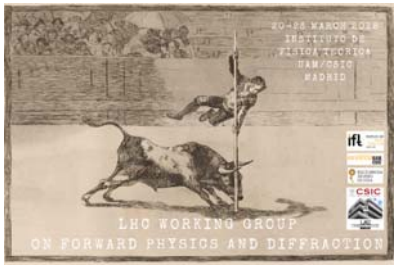

The distribution functions of quarks and diquarks in a colliding proton, for arbitrary n, are:

$$u_{uu}(x,n) = C_{uu}x^{\alpha_R-2\alpha_B+1}(1-x)^{-\alpha_R+\frac{4}{3}(n-1)},$$

$$u_{ud}(x,n) = C_{ud}x^{\alpha_R-2\alpha_B}(1-x)^{-\alpha_R+n-1},$$

$$u_{u}(x,n) = C_{u}x^{-\alpha_R}(1-x)^{\alpha_R-2\alpha_B+n-1},$$

$$u_{d}(x,n) = C_{d}x^{-\alpha_R}(1-x)^{\alpha_R-2\alpha_B+1+\frac{4}{3}(n-1)},$$

$$u_{s}(x,n) = C_{d}x^{-\alpha_R}(1-x)^{\alpha_R-2\alpha_B+n-1}.$$

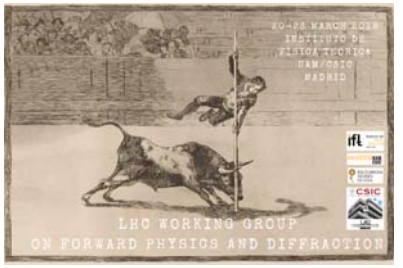

The distribution functions of quarks and diquarks in a colliding π^-, for arbitrary n, are:

$$u_d(x,n) = u_{\bar{u}}(x,n) = C_d x^{-\alpha_R}(1-x)^{-\alpha_R+n-1},$$

$$u_u(x,n) = u_{\bar{d}}(x,n) = C_u x^{-\alpha_R}(1-x)^{-\alpha_R+n-1}\left[1-\delta\sqrt{1-x}\right],$$

$$n > 1,$$

$$u_{\bar{s}}(x,n) = C_{\bar{s}} x^{-\alpha_R}(1-x)^{n-1}, \qquad n > 1$$

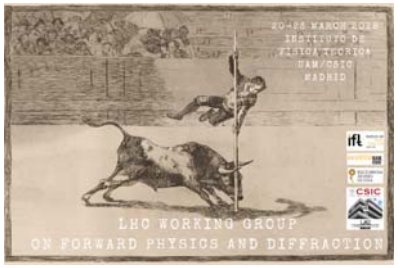

For the φ-meson production, the quark fragmentation functions are obtained by using the Reggeon counting rules and the simplest extrapolation:

$$G_u^{\varphi} = G_d^{\varphi} = G_{\bar{u}}^{\varphi} = G_{\bar{d}}^{\varphi} = a_{\varphi} \cdot (1-z)^{\lambda - \alpha_R - 2\alpha_{\varphi} + 2},$$

$$G_s^{\varphi} = G_{\bar{s}}^{\varphi} = a_{\varphi} \cdot (1-z)^{\lambda - \alpha_{\varphi}}.$$

The diquark fragmentation functions into φ-mesons have the form:

$$G_{uu}^{\varphi} = G_{ud}^{\varphi} = a_{\varphi} \cdot (1-z)^{\lambda + \alpha_R - 2(\alpha_R + \alpha_{\varphi})}$$

where the parameter λ takes the value $\lambda = 0.5$, and $\alpha_R = 0.5$, and $\alpha_{\varphi}=0$. are the intercepts of the ρ and φ Regge trajectories, respectively.

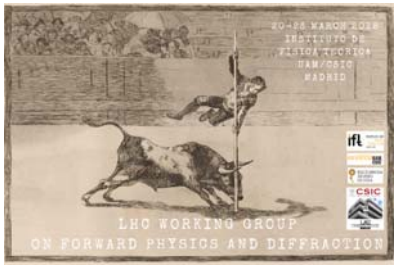

The only unknown parameter in this analysis is α_φ, that represents the φ density in the central region of one Pomeron.

Its value sets the absolute normalization of the φ production cross section.

The value of α_φ is universal in the sense that it does not depend, neither of the energy, nor of the beam of the collision.

This value has been fixed, by simultaneously describing in a reasonable way most of the experimental data on φ production from pion and proton beams, to be $\alpha_\varphi = 0.11$.

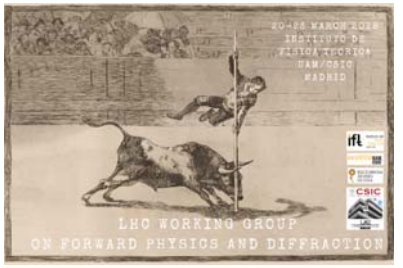

In the case of interaction with a nuclear target, the Gribov-Glauber theory is used (superposition of interactions with different numbers of target nucleons).

Let $W_{pA}(\nu)$ be the probability for the inelastic interactions of the proton with ν nucleons of the target, and σ_{prod}^{pA} the total cross section of secondary production in a proton-nucleus collision:

$$W_{pA}(\nu) = \sigma^{(\nu)} / \sigma_{prod}^{pA} \ ,$$

$$\sigma^{(\nu)} = \frac{1}{\nu!} \int d^2b \cdot [\sigma_{inel}^{pN} \cdot T(b)]^{\nu} \cdot e^{-\sigma_{inel}^{pN} \cdot T(b)}$$

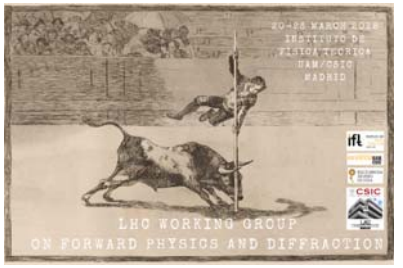

$$\sigma_{prod}^{pA} = \int d^2b \cdot \left(1 - e^{-\sigma_{inel}^{pN} \cdot T(b)}\right),$$

where **T(b)** is the profile function of the nuclear target:

$$T(b) = A \int_{-\infty}^{\infty} dz \cdot \rho(b, z),$$

with $\rho(b,z)$, the one-particle nuclear density.

The average value of ν has the form:

$$\langle \nu \rangle = \frac{A \cdot \sigma_{inel}^{pp}}{\sigma_{prod}^{pA}} .$$

$$\langle \nu \rangle_{p+Pb} \approx 7.9.$$

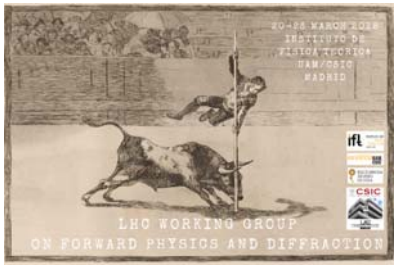

It is important to take into account all diagrams featuring all possible configurations of Pomerons and their respective permutations.

The quark and diquark distributions and fragmentation functions are identical to those in the case of p-nucleon interactions.

The growth of the total number of interacting Pomerons is given by

$$\langle k \rangle_{pA} \sim \langle \nu \rangle_{pA} \langle k \rangle_{pN}$$

(about 4 for heavy nuclei at energies in the range 10^2-10^3 GeV)

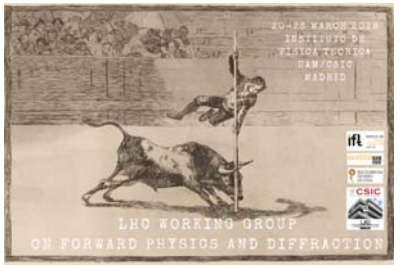

In the case of nucleus-nucleus scattering in the projectile-fragmentation region, the approach in which a beam of independent nucleons interacts with the target is used (rigid-nucleus approximation in Glauber's theory).

In the target –fragmentation region, the set of independent target nucleons interacts with a projectile nucleus.

These two contributions coincide in the midrapidity region.

This approach successfully describes $\pi^{\pm}$, $K^{\pm}$, p, and $\bar{p}$, production in PbPb collisions at 158 GeV/c per nucleon.

In the present study, we use the Pomeron parameters, and the distribution and fragmentation functions shown above.

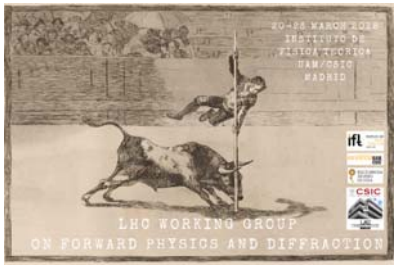

III. Description of the experimental data on hadroproduction of φ-mesons on proton target:

We compare the results of the QGSM calculations with the experimental data on φ inclusive cross sections in πp and pp collisions at different energies up to the LHC range.

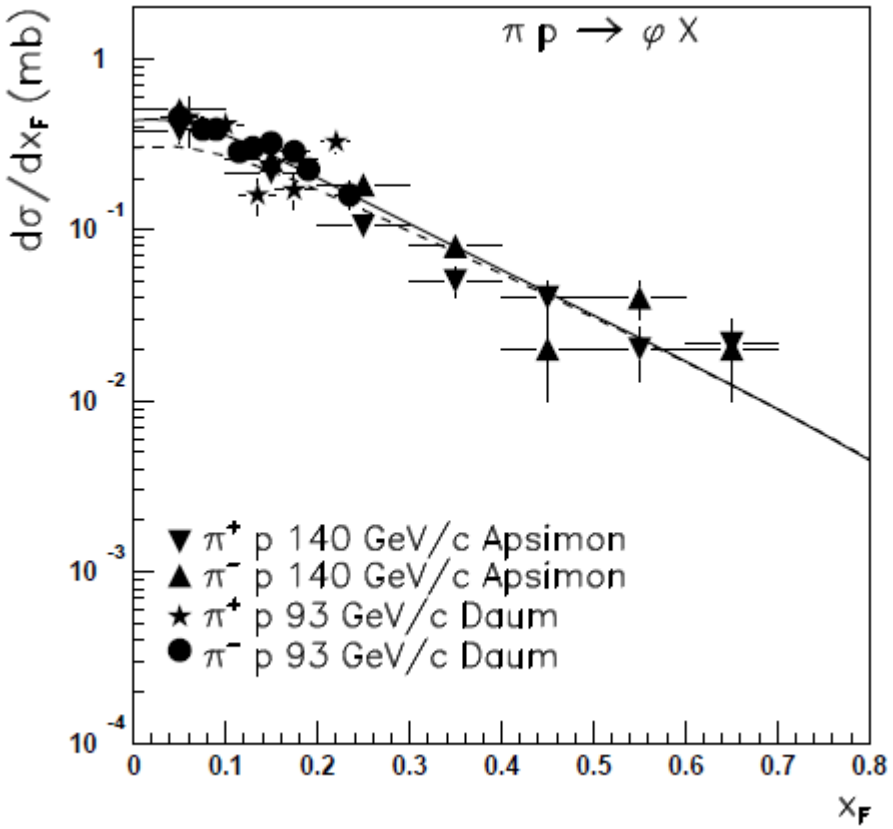

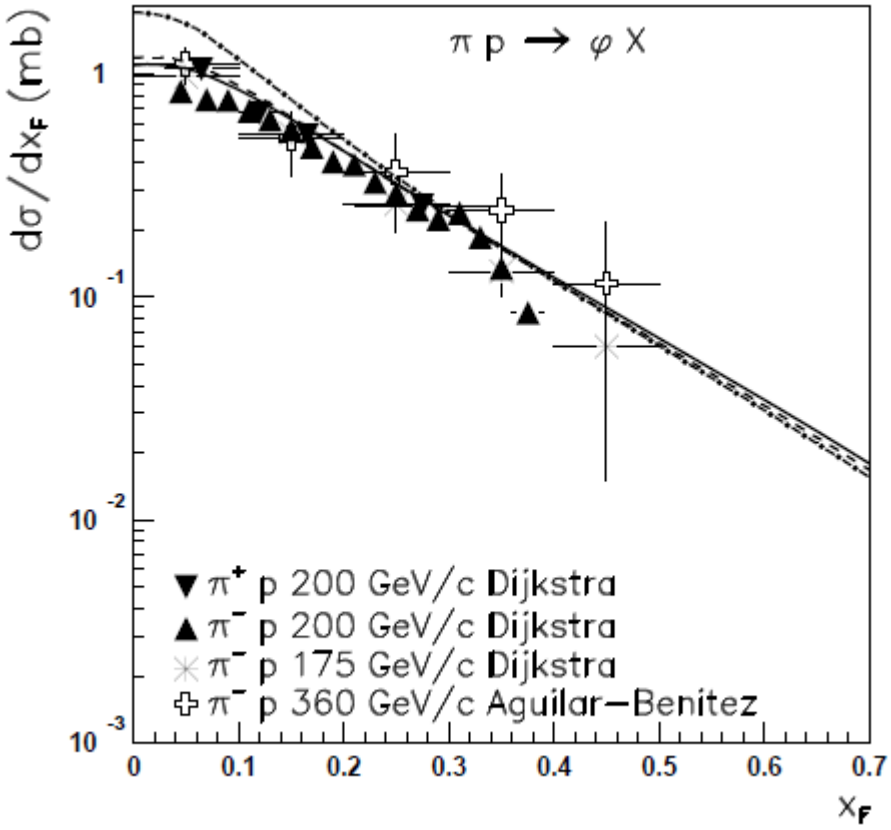

Experimental data on x_F-spectra of φ-mesons in $\pi^{\pm}$p collisions at different energies, compared to the corresponding QGSM results

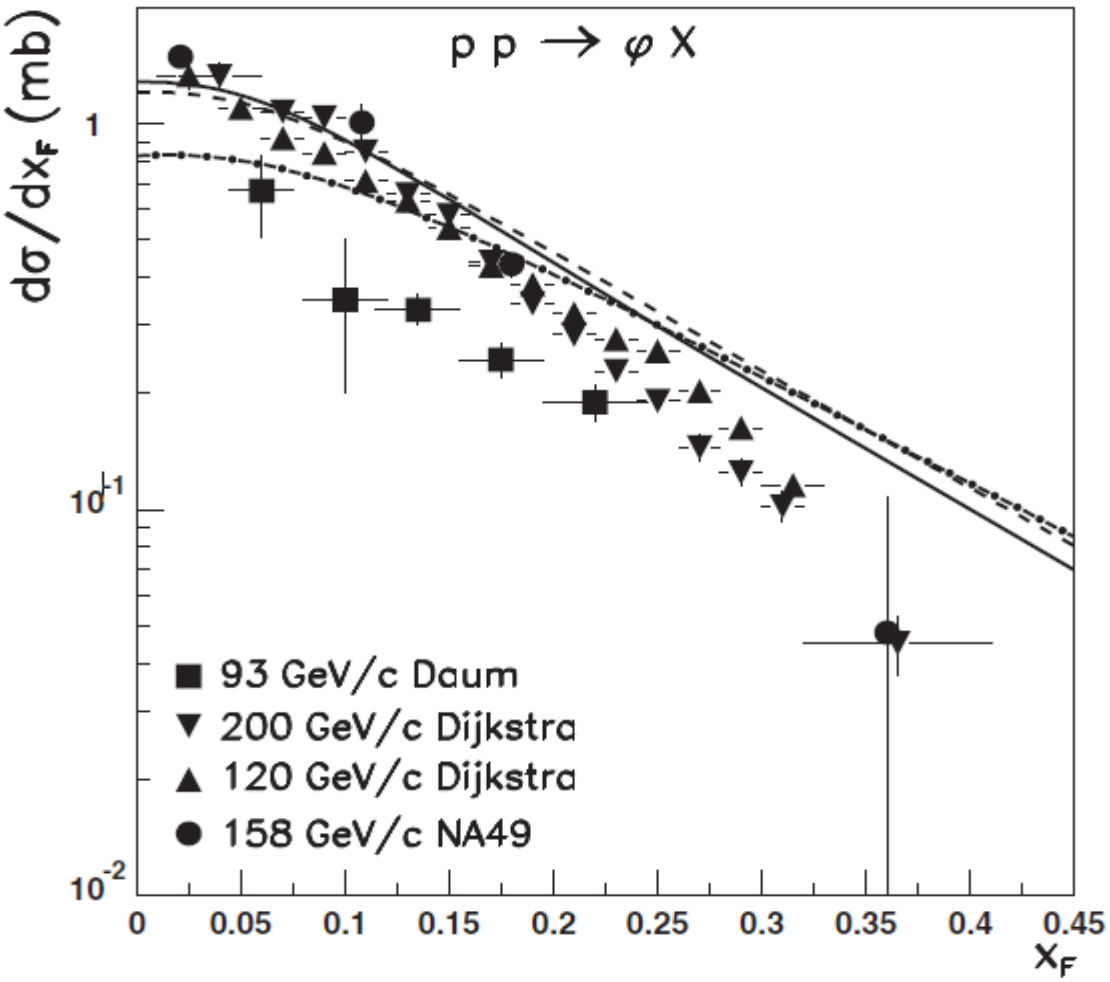

Experimental data on x_F-spectra of φ-mesons in pp collisions at 93, 120, 158, and 200 GeV/c, compared to the corresponding QGSM results at 93, 158, and 200 GeV/c.

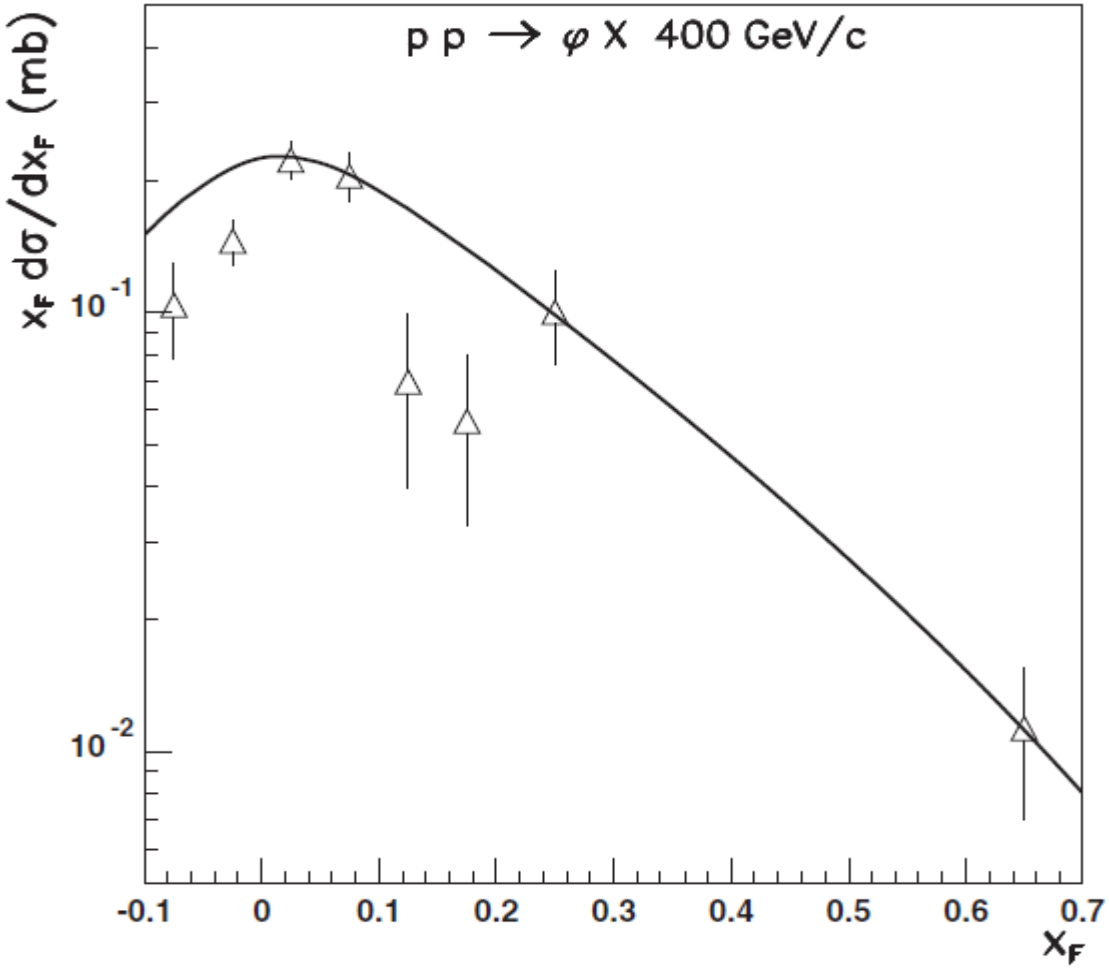

Experimental data on x_F-spectra of φ-mesons in pp collisions at 400 GeV/c (LEBC-EHS Collaboration, ZPC**50** (1991), 405), compared to the corresponding QGSM results.

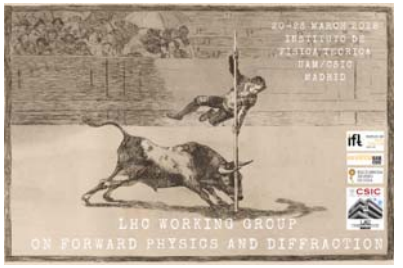

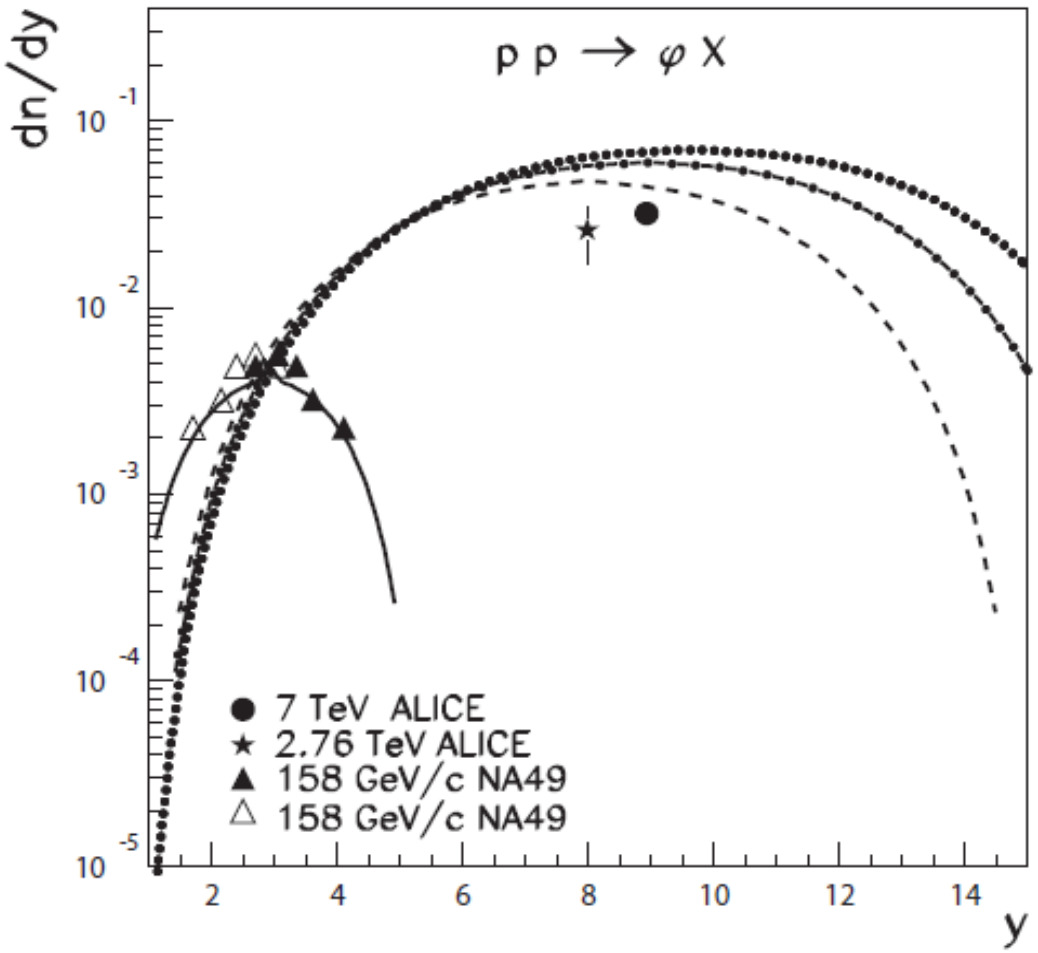

Experimental data on y-spectra dn/dy of φ-mesons in pp collisions at 158 GeV/c (LEBC-EHS Collaboration, ZPC**50** (1991), 405), compared to the corresponding QGSM results.

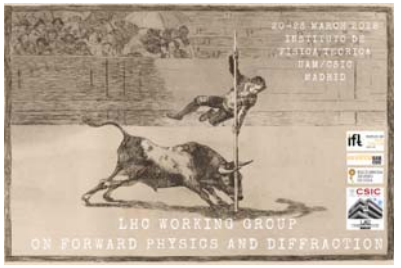

The QGSM curves for 2.76 TeV (dashed) and 7 TeV (dashed-dotted) were predictions, published previously to the experimental points. The dotted curve is the QGSM prediction for 14 TeV.

Generally, the QGSM description of the experimental data in the considered energy region shown in these figures is consistent.

The description of the large x_F region is rather good in the case of πp collisions, while for the pp collisions the only point at 400 GeV/c is in agreement with the theoretical curve.

The QGSM dn/dy curves are remarkably higher than the experimental points, that were measured at $p_T \geq 0.4\ GeV/c$ and extrapolated to $p_T = 0$.

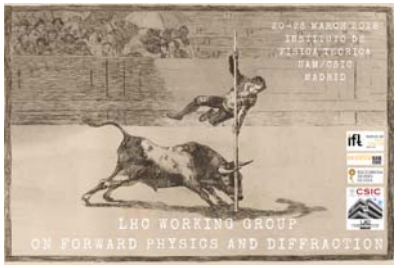

IV. Production of φ-mesons on nuclear targets up to the RHIC energies:

We analyze experimental data by the HERA-B Collaboration on φ-meson production in collisions of protons with C, Ti, and W nuclei.

The experimental data (HERA-B Collaboration, EPJC50 (2007), 315) were integrated over the whole range of p_T at. $\sqrt{s} = 41.6$ GeV.

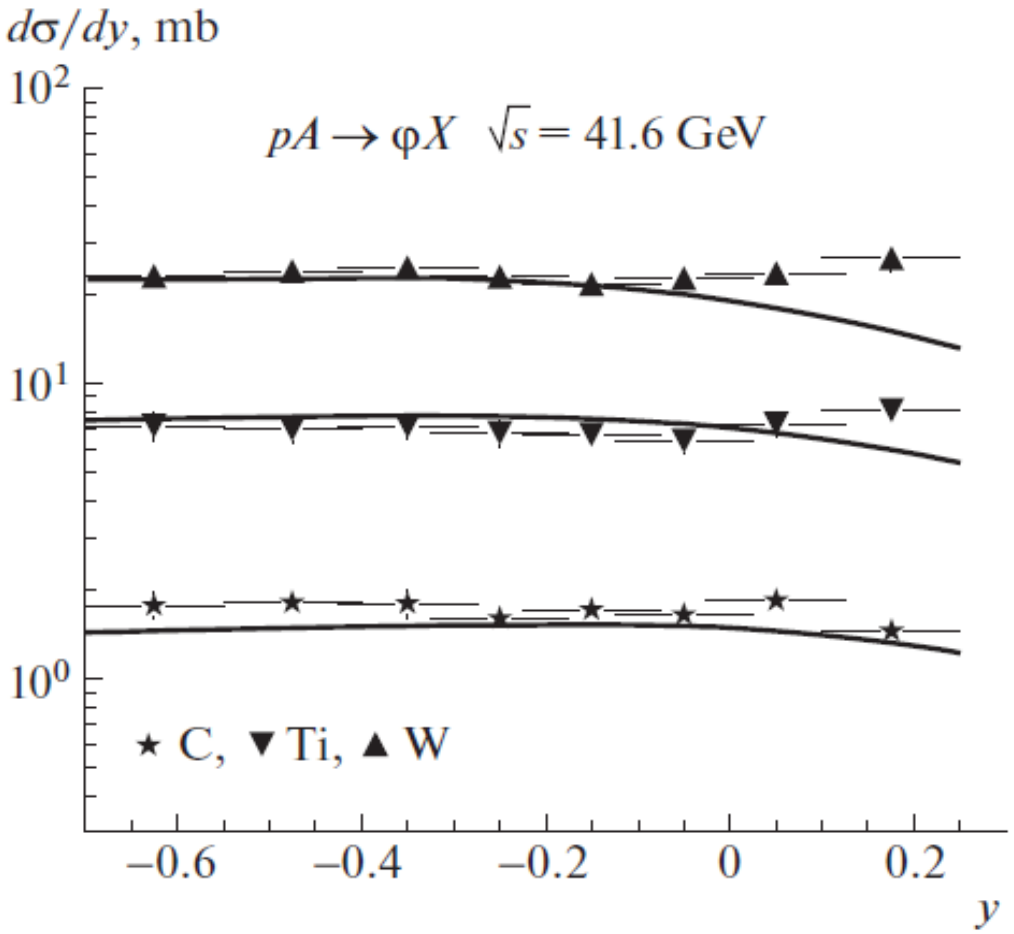

Experimental data on the y dependence of the cross sections for φ-meson production, dn/dy, in pA collisions, where A=C,Ti, and W, at the energy $\sqrt{s}$ =41.6 GeV, compared to the results of the corresponding QGSM calculations.

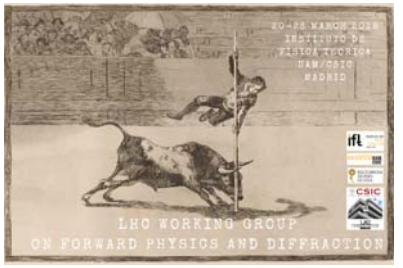

Reaction	Experimental data, $d\sigma_{pA}/dy$, $(\|y\| \leq 0.5)$, mb	QGSM
p + C	1.74 ± 0.15	1.5
p + Ti	6.85 ± 0.7	7.1
p + W	23.5 ± 2.1	19.1

Experimental data on the y dependence of the cross sections for φ-meson production, dn/dy, in pA collisions at $\sqrt{s}$ =41.6 GeV, and results of the corresponding QGSM calculations.

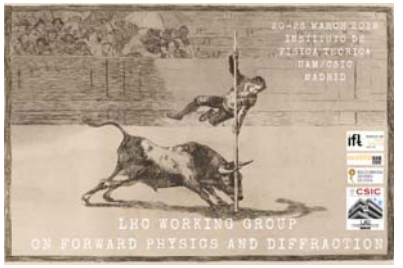

The QGSM results compare reasonably with the HERA-B experimental data everywhere, with the exception of some discrepancies in the positive region of $y \geq 0$, especially for the W nucleus.

In the case of φ-meson production, the inelastic-screening effects are not noticeable in the energy region up to the RHIC energies, but they will be significant at the LHC energies.

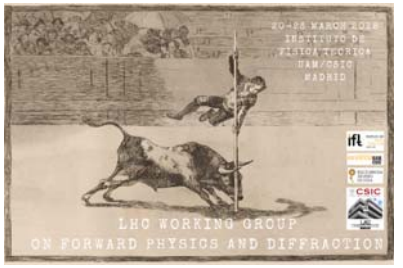

V. Rapidity spectra of φ-mesons in pPb and PbPb collisions at LHC energies:

We analyze φ-meson production on nuclear targets at LHC energies, by taking into account the importance of the inelastic-shadowing effects at these energies.

The inclusive density for the production of secondary particles exhibits significant saturation effects, both in pPb and PbPb collisions, starting from RHIC energies (experimentally confirmed), even for φ-meson production.

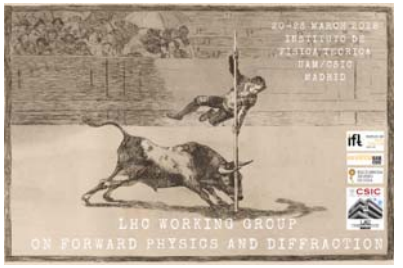

Saturation effects can be explained by corrections for inelastic shadowing connected to the multipomeron interactions, which are negligible at low energies, but become more and more important as the initial energy grows.

In the case of interaction with nuclei, the mean number of Pomerons is large, and even at RHIC and LHC energies, their interactions become significant.

The percolation approach can be used to calculate inclusive densities and multiplicities in pA and heavy ion collisions, with accounting for the inelastic shadowing. The results of these calculations are in agreement with experimental data over a broad energy region.

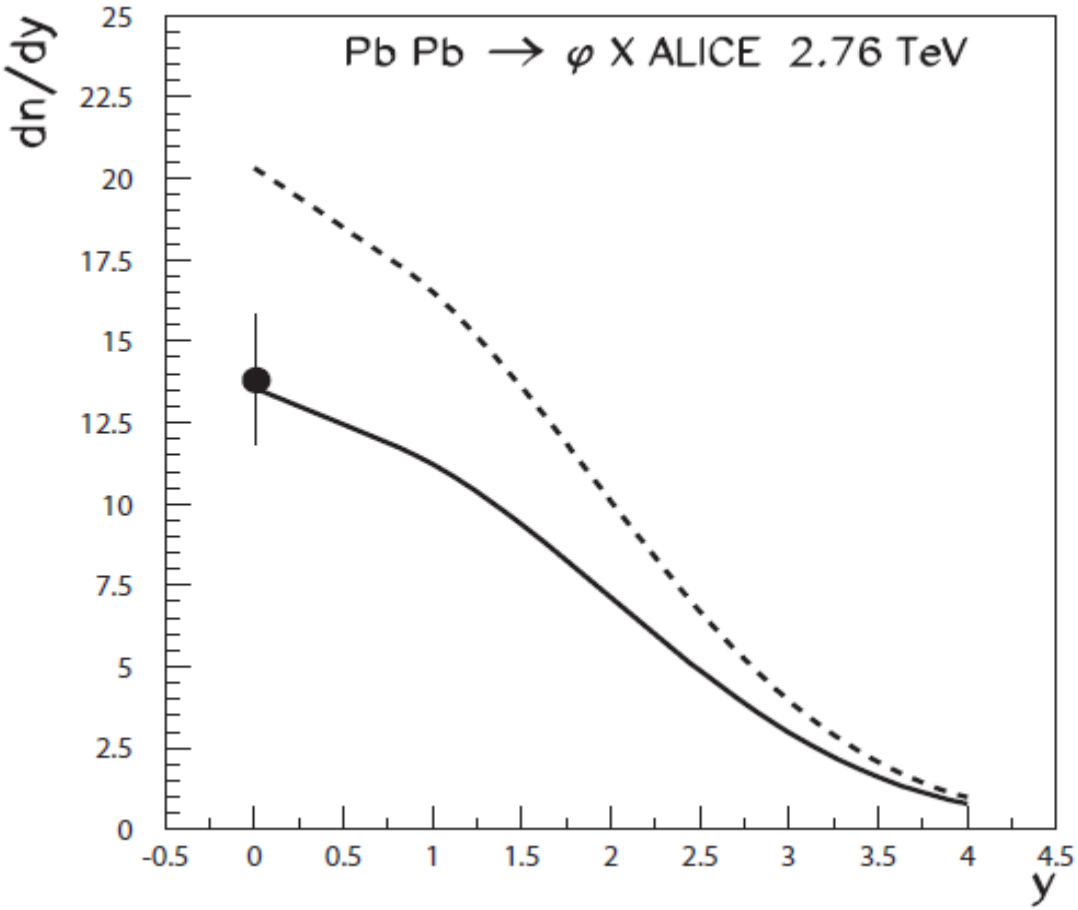

QGSM result for the rapidity dependence of the density for φ-meson production, dn/dy, in central PbPb collisions at $\sqrt{s} = 2.76\ TeV$, with (full) and without (dashed curve) inelastic shadowing.

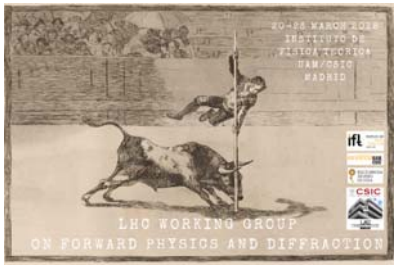

The QGSM result for the rapidity dependence of the density for φ-meson production, dn/dy, in central PbPb collisions at $\sqrt{s}$ =2.76 TeV, appeared as a prediction, before the experimental point by ALICE Collaboration was published in 2015 (PRC91 (2015), 024609).

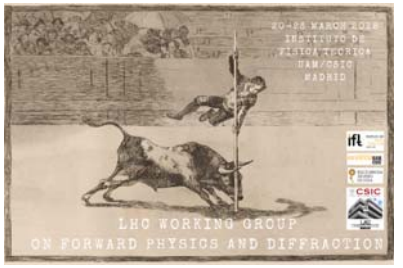

Reactions	Centrality	Energy $\sqrt{s}, TeV$	Experimental data dn/dy $(\|y\| \leq 0.5)$	QGSM
Pb + Pb	0–5%	2.76	$13.8 \pm 0.5 \pm 1.7 \pm 0.1$ [59]	13.57
p + Pb	NSD	5.02	$0.1344 \pm 0.005 \pm 0.0069 \pm 0.0081$ [60]	0.14

Comparison of the QGSM results for dn/dy for φ-meson production in PbPb collisions (|y|≥0.5) at $\sqrt{s} = 2.76\,TeV$, and for the pPb minimum bias spectrum normalized to the fraction of non-single-diffraction (NSD) events at $\sqrt{s} = 5.02\,TeV$, with the corresponding experimental points by the ALICE Collaboration (PRC**91** (2015), 024609, and EPJC**76** (2016), 245).

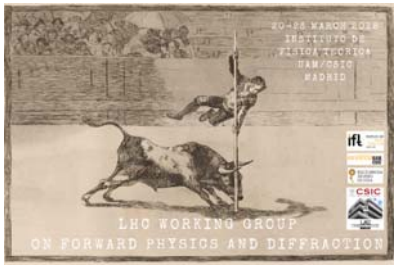

At $\sqrt{s}$ = 2.76 TeV, the inelastic-shadowing effect reduces the value of dn/dy (|y|≤0.5) for φ-meson production by about 1.5.

At this energy, the $\pi^{\pm}$, $K^{\pm}$, p, and $\bar{p}$ spectra decrease by a factor of about two, because of a larger contribution of inelastic shadowing.

Secondary φ-meson production in pA and AA collisions, with accounting for inelastic-shadowing effects, can be calculated without any additional parameter with respect to the corresponding calculation for pp collisions.

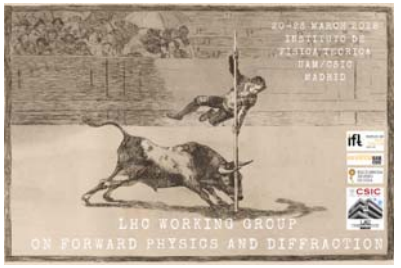

VI. Conclusions (1)

The Quark-Gluon String Model is a phenomenological model based on rigorous theoretical background.

The QGSM provides a reasonable description of both the x_F and y spectra of φ-production for the interaction of different hadron beams with a nucleon target in a wide energy region.

The QGSM predictions for the dn/dy density in pp collisions at LHC energies are compared with recent experimental data at $\sqrt{s}$ = 2.76 and 7 TeV in the midrapidity region.

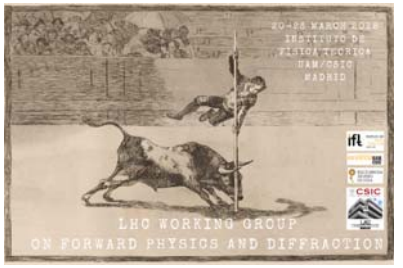

VI. Conclusions (2)

The QGSM provides a reasonable description of φ-production in both pA and AA collisions up to the RHIC energies without including inelastic-shadowing effects.

The inelastic-shadowing effect is markedly weaker in the case of φ-production than for production of $\pi^{\pm}$, $K^{\pm}$, p, and $\overline{p}$, becoming observable only at higher energies $\sqrt{s}$ ≥ 0.9 TeV.

This behaviour can be explained by the fact that the mass of the s quark is not negligible.

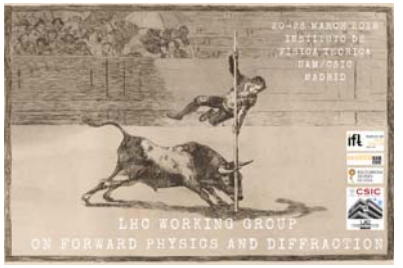

VI. Conclusions (3)

It would be important to measure φ-production at LHC in pp collisions for a wide region of rapidity, in particular in the forward direction, to establish the shape of the rapidity dependence, dn/dy.

This would be useful to fix the parametrization of the fragmentation functions for φ-production in the whole rapidity range.

Those data would also help in analyzing the dependence of $<p_T>$ vs energy, that in QGSM determines the growth of cross sections and densities dn/dy, from pp to PbPb.